Journal of Materials Chemistry A

PAPER

View Article Online
View Journal | View Issue

Cite this: J. Mater. Chem. A, 2014, 2, 12940

Evolution of the electrochemical capacitance of transition metal oxynitrides with time: the effect of ageing and passivation

Olga Kartachova,[a] Ying Chen,[a] Robert Jones,[b] Yanhui Chen,[c] Hongzhou Zhang[c] and Alexey M. Glushenkov*[ad]

Received 15th January 2014
Accepted 1st June 2014

DOI: 10.1039/c4ta00220b

www.rsc.org/MaterialsA

A number of transition metal nitrides and oxynitrides, which are actively investigated today as electrode materials in a wide range of energy conversion and storage devices, possess an oxide layer on the surface. Upon exposure to ambient air, properties of this layer progressively change in the process known as "ageing". Since a number of electrochemical processes involve the surface or sub-surface layers of the active electrode compounds only, ageing could have a significant effect on the overall performance of energy conversion and storage devices. In this work, the influence of the ageing of tungsten and molybdenum oxynitrides on their electrochemical properties in supercapacitors is explored for the first time. Samples are synthesised by the temperature-programmed reduction in NH_3 and are treated with different gases prior to exposure to air in order to evaluate the role of passivation in the ageing process. After the synthesis, products are subjected to controlled ageing and are characterised by low temperature nitrogen adsorption, X-ray photoelectron spectroscopy and transmission electron microscopy. Capacitive properties of the compounds are evaluated by performing cyclic voltammetry and galvanostatic charge and discharge measurements in the 1 M H_2SO_4 electrolyte.

1. Introduction

In recent years, transition metal nitrides and oxynitrides have been widely investigated as candidates for applications in the energy conversion and storage devices due to their unique physico-chemical properties such as high intrinsic conductivity, electrochemical and Pt-like electrocatalytic activities, as well as the resistance to corrosion.[1–36] The range of devices they can be potentially used in includes lithium-ion batteries, electrochemical supercapacitors, dye-sensitised solar cells, metal–air batteries and fuel cells. For instance, compounds such as CrN,[2] CoN (ref. 3 and 4) and $(Ni_{0.33}Co_{0.67})N$ (ref. 5) nanoparticles as well as thin films of VN,[6] CrN,[7] Co_3N,[8] Fe_3N,[8] RuN,[9] Mn_3N_2 (ref. 10) and V_2ON (ref. 11) have demonstrated reversible capacity values between 323 mA h g^{-1} for Fe_3N (ref. 8) and 1200 mA h g^{-1} for CrN (ref. 7) through a conversion reaction mechanism as anode materials for lithium-ion batteries. In supercapacitors, transition metal nitrides and oxynitrides have shown good rate capabilities, as opposed to many transition metal oxides which suffer from poor intrinsic conductivity, with typical specific capacitance values between 30 and 350 F g^{-1}.[9,12–26] MoW(N,O) has demonstrated the ability to operate at a current as high as 20 A g^{-1}, still retaining 43% of its initial capacitance measured at 0.05 A g^{-1},[14] while TiN–VN core–shell mesoporous fibres have retained 64% of the initial capacitance upon increasing the current load from 2 to 10 A g^{-1}.[15] Dye-sensitised solar cells with electrocatalytic counter-electrodes containing Mo_2N,[27] W_2N,[27] VN,[28] MoN,[29] WN (ref. 29) or Fe_2N (ref. 29) have shown up to 92% of the photovoltaic performance of the solar cells with platinum counter-electrodes.[27–29] Furthermore, TiN,[30–32] TaO_xN_y,[33] CoWON,[34] Mo(N,O)[35] and Co_3Mo_3N (ref. 36) appear promising as electrocatalysts for the oxygen reduction reaction.

In the energy conversion and storage devices, a number of electrochemical and electrocatalytic processes such as the pseudocapacitive charge storage or oxygen reduction reaction often involve the surface or sub-surface layers of the active electrode materials. In fact, it has been proposed that the origin of the specific capacitance of vanadium nitride could be attributed to the presence of vanadium oxides or oxynitrides on the surface, which participate in faradaic processes with ions from the electrolyte.[26] Furthermore, the mechanism of the oxygen reduction reaction is influenced by the presence of the

[a]Institute for Frontier Materials (IFM), Deakin University, Waurn Ponds, VIC 3216, Australia. E-mail: alexey.glushenkov@deakin.edu.au; Fax: +61 3 5227 1103; Tel: +61 3 5227 2931

[b]Centre for Materials and Surface Science, Department of Physics, La Trobe University, VIC 3086, Australia. E-mail: R.Jones@latrobe.edu.au; Fax: +61 3 9479 1552; Tel: +61 3 9479 2646

[c]School of Physics and Centre for Research on Adaptive Nanostructures and Nanodevices (CRANN), Trinity College Dublin, Dublin 2, Ireland. E-mail: hozhang@tcd.ie; Fax: +353 1 896 3033; Tel: +353 1 896 4655

[d]Melbourne Centre for Nanofabrication, 151 Wellington Rd, Clayton, VIC 3168, Australia

active sites for O_2 adsorption and water desorption on the surface of the nitride or the oxynitride electrocatalyst.[32–34] The properties and composition of the surface are therefore critical for the performance of these compounds as electrode materials.

It has been demonstrated, in the field of catalysis, that a number of transition metal nitrides and oxynitrides possess an oxide layer on the surface and properties of this layer change with time.[37–39] For instance, the surface of the passivated tungsten oxynitride becomes progressively covered with tungsten trioxide WO_3 upon exposure to air.[37] Furthermore, in the case of molybdenum oxynitrides,[38,39] an increase of the oxygen content has been revealed by the chemical analysis[38,39] or X-ray photoelectron spectroscopy (XPS) measurements[39] after storing the samples in ambient air. Interestingly, no variations in the bulk structure of the materials have been detected on the X-ray diffraction (XRD) spectra,[37–39] indicating that ageing involves the surface or sub-surface layers only. This evolution of the surface composition of transition metal nitrides and oxynitrides with time remains almost unexplored in the field of the energy conversion and storage devices. Despite the promise of these materials, there are no studies, to the best of our knowledge, correlating ageing of nitrides and oxynitrides with changes in their electrochemical properties.

Furthermore, a number of these compounds are usually passivated (*i.e.* exposed to a stream of a gas containing a small amount of oxygen) prior to the exposure to air in order to form a protective oxide layer and avoid the strong oxidation of the surface. The role of passivation in the ageing process is not understood well, and the changes in the passivated materials remain largely unknown. It is, in our view, important to investigate the influence of ageing and passivation on the electrochemical properties of transition metal nitrides and oxynitrides in order to determine the optimal synthesis and storage conditions, as changes of the surface properties could have an influence on their performance in the energy conversion and storage devices. Such a study may also be relevant to other related materials such as transition metal carbides, which have physico-chemical properties similar to those of nitrides and are also emerging as promising electrode materials. For example, transition metal carbide electrodes have been recently reported to have impressive capacitances in supercapacitors,[40] with volumetric capacitance values exceeding those of the activated graphene electrodes.

In this article, the influence of ageing is investigated by comparing the performance of the fresh and aged molybdenum and tungsten oxynitrides as electrode materials in supercapacitors. Molybdenum and tungsten oxynitrides are synthesised by a temperature-programmed reduction in ammonia gas and exposed to ambient air for different periods. In order to study the role of passivation in the aging process, passivated and non-passivated tungsten oxynitrides are produced. Samples are characterised by low temperature nitrogen (N_2) adsorption, X-ray photoelectron spectroscopy (XPS) and transmission electron microscopy (TEM). The effect of ageing on the electrochemical performance in supercapacitors is evaluated by performing cyclic voltammetry and galvanostatic charge and discharge measurements in 1 M H_2SO_4 solution.

2. Experimental

2.1 Synthesis

Molybdenum and tungsten oxynitride samples were prepared by a temperature-programmed reduction of the corresponding oxide precursors (MoO_3 and WO_3, respectively). The detailed temperature-programmed reduction procedure is described elsewhere.[35] In brief, 0.5 g of the oxide precursor were heated in ammonia flow (0.2 l min^{-1}). The temperature was raised to 700 °C at a rate of 3 °C min^{-1} and kept stable for 2 h. Subsequently, the sample was allowed to cool down to room temperature while the ammonia flow was maintained. The synthesised samples are further denoted as Mo(N,O) and W(N,O). In the present experiment, the synthesised molybdenum and tungsten oxynitride samples were treated with high-purity Ar (Coregas, Australia) prior to the exposure to air for one hour. In order to study the effect of room temperature oxidation (ageing), the synthesised samples were stored in open containers for periods up to 48 days in a drawer of a cabinet in the laboratory. Additionally, to evaluate the influence of passivation on ageing of the oxynitrides and its effect on the electrochemical properties, some synthesised tungsten oxynitride samples are passivated with a special gas mixture (Ar + 0.1 vol% O_2) for one hour prior to the exposure to air.

Samples W0–W48 correspond to the non-passivated tungsten oxynitride and the samples Mo0–Mo48 correspond to the non-passivated molybdenum oxynitride, exposed to ambient air for different periods. Samples WP0–WP48 denote the passivated tungsten oxynitride (refer Table 1).

2.2 Nitrogen adsorption and TEM analysis

Low temperature nitrogen adsorption measurements were performed on powder samples using a Micromeritics Tristar 3000. The surface area was calculated from the low temperature adsorption isotherm by the Branauer–Emmett–Teller (BET) method. The pore size distribution was evaluated using the Barrett–Joyner–Halenda (BJH) method. TEM characterisation was performed with an FEI Titan, operating at an accelerating voltage of 300 kV. Energy filtered TEM (EFTEM) imaging was performed using the three window method.

2.3 Electrochemical testing

Electrochemical performance of the samples in supercapacitors was evaluated by cyclic voltammetry and galvanostatic charge

Table 1 Description of tungsten oxynitride (W0–W48 and WP0–WP48) and molybdenum oxynitride (Mo0–Mo48) samples exposed to air for different periods

Sample	Storage period (days)	Sample	Storage period (days)	Sample	Storage period (days)
W0	0 (fresh)	Mo0	0 (fresh)	WP0	0 (fresh)
W5	5	Mo21	21	WP5	5
W21	21	Mo35	35	WP21	21
W48	48	Mo48	48	WP48	48

Table 2 Weights of the active materials on tungsten oxynitride (W0–W48, WP0–WP48) and molybdenum oxynitride (Mo0–Mo48) electrodes

Sample	Weight of the active material[a] (mg)	Sample	Weight of the active material (mg)	Sample	Weight of the active material (mg)
W0	2.38	Mo0	2.33	WP0	2.14
W5	2.31	Mo21	2.35	WP5	2.02
W21	2.32	Mo35	2.36	WP21	2.27
W48	2.4	Mo48	2.48	WP48	2.02

[a] Total measurement uncertainty is 0.035 mg.

and discharge experiments in the 1 M H_2SO_4 electrolyte. Electrodes were prepared by coating a slurry, composed of the active material (90 wt%), carbon nanopowder (Sigma-Aldrich, #699632) (5 wt%), poly(vinylidene)fluoride (PVDF, Sigma-Aldrich) (5 wt%) and *N*-methyl-2-pyrrolidone (NMP, Sigma-Aldrich, anhydrous, 99.5%) as a solvent, onto titanium foils. The coated foils were dried in a vacuum at 90 °C in the conventional oven overnight. Pt wires were used as counter electrodes and Ag/AgCl electrodes were used as reference electrodes. The electrochemical cells were filled with the electrolyte under vacuum. In order to accurately compare the cyclic voltammetry measurements of the samples, electrodes with nearly identical weights were selected (Table 2).

2.4 XPS analysis

Prior to the use of electrodes in the electrochemical experiments, X-ray photoelectron spectra were acquired from the electrodes with a Kratos AXIS Nova instrument (Kratos Analytical Ltd, Manchester, UK) equipped with a monochromated Al Kα X-ray source ($h\nu = 1486.6$ eV) operating at 150 W. Mo 3d and W 4f spectra were recorded at a pass energy of 20 eV and 0.1 eV per step. The pressure was below 6×10^{-9} torr. The binding energy measured for the dominant component of the C 1s photoemission was 284.4 eV, which is typical of graphitic carbon.[41]

3. Results

3.1 Characterisation and electrochemical properties of the non-passivated tungsten and molybdenum oxynitrides

3.1.1 Characterisation of tungsten oxynitride. Low temperature N_2 adsorption and desorption isotherms for the non-passivated tungsten oxynitride samples (Fig. 1a) present a hysteresis and correspond to type IV. BET surface areas of 54, 42, 44 and 48 $m^2\ g^{-1}$ were measured for samples W0, W5, W21 and W48, respectively. Interestingly, after an initial drop of the surface area, no further decrease is observed upon progressive ageing of the samples, contrary to the previous reports.[37–39] In the present case, the maximum of the pore size distribution of the as-synthesised compound is centred around 5 nm (Fig. 1b). After the exposure to air for 5 days, the maximum around 5 nm disappears, giving rise to two maxima centred around 3 and 7 nm, respectively. Upon ageing, the proportion of mesopores with 3 nm diameter increases, while pores with 7 nm diameter progressively disappear. Low temperature N_2 adsorption results could therefore indicate that exposure of the samples to ambient air leads to a progressive decrease of the diameters of mesopores.

The surface composition of the tungsten oxynitride samples is determined from their W 4f photoemission spectra, shown in Fig. 2. Acceptable fits to the experimental data were obtained using two doublets, each with a separation of about 2 eV between the $4f_{7/2}$ and $4f_{5/2}$ component peaks (Table 3). The principal ($4f_{7/2}$) peak of the doublet at higher binding energy is centred at approximately 35.7 eV for each sample, which is close to the range of values reported for WO_3.[37,42] Consequently, this component is labelled W^{6+}, and is evidence for the presence of tungsten trioxide. The $4f_{7/2}$ peak of the doublet at lower binding energy is centred at approximately 32.5 eV, from which it is concluded that a second tungsten phase is also present on the sample surfaces: one with W in a lower oxidation state. The identity of this phase is uncertain, as the measured binding energies fall between those reported for the mixed nitride, W_2N + WN (32.0 eV),[37] and WO_2 (33.0 eV),[42] and so the component is labelled $W^{\delta+}$, where $\delta < 6$ (Fig. 2). When comparing the $W^{6+}/W^{\delta+}$ ratios for the fresh and aged samples (Table 4), it could be noted that upon exposure to air, the concentration of WO_3 species on the surface increases. Interestingly, after an initial change of the $W^{6+}/W^{\delta+}$ ratio from 0.47 to 0.75, no further significant increase of the ratio is observed. This result could indicate that tungsten oxynitride forms an oxide layer on the surface shortly after the exposure to ambient air.

In order to investigate the oxidation of the surface of tungsten oxynitride samples in more detail, advanced TEM characterisation of the aged sample (W48) was attempted. Bright-field TEM (Fig. 3a) as well as high-angle scanning transmission electron microscopy (STEM) images (Fig. 3b) demonstrate that the material maintains the porous morphology after 48 days of exposure to ambient air. EFTEM maps of oxygen and nitrogen (Fig. 3a) indicate that these elements are distributed throughout the samples and therefore confirm that the synthesised material is oxynitride, similar to the previously reported data for the fresh tungsten oxynitride.[13] Upon analysis of the variations of the O/N ratio throughout the sample in the STEM mode (line scans), it could be observed that the distribution of O and N elements is not homogenous (Fig. 3b). It is, however, not possible to determine the locations of predominant oxidation. Conflicting trends in the variations of the O/N ratio were observed in a number of attempted line scans. Comparing the results with the previously reported TEM images of the

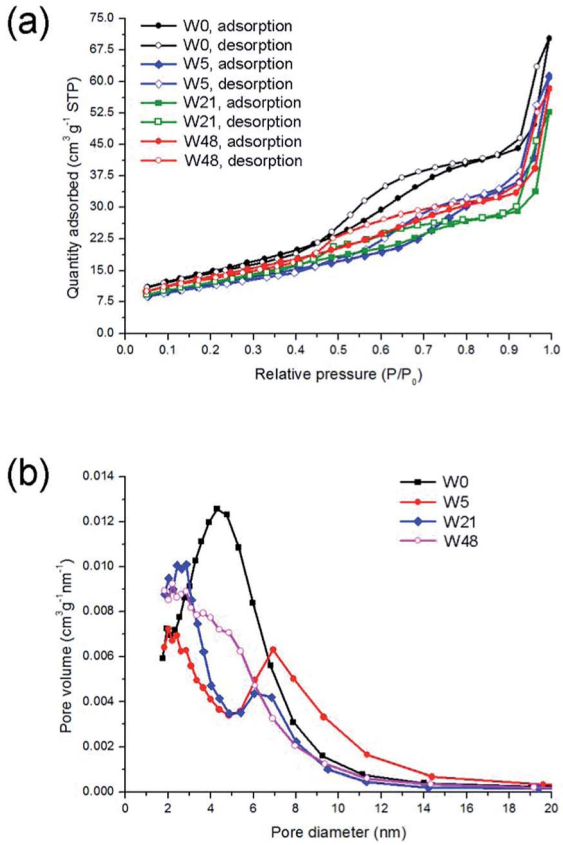

Fig. 1 Nitrogen adsorption and desorption isotherms (a) and pore size distributions (b) for the non-passivated tungsten oxynitride samples.

as-synthesised tungsten oxynitride,[13] any obvious difference between the fresh and aged samples is difficult to argue. We have therefore concluded that the scale of changes upon ageing occurs within a fine range of about 1 nm and could not be monitored reliably with the TEM equipment available to us.

3.1.2 Electrochemical properties of tungsten oxynitride. Cyclic voltammetry (CV) curves of tungsten oxynitride samples in the 1 M H_2SO_4 electrolyte (Fig. 4a) show a nearly ideal rectangular CV curve for the as-synthesised sample (W0), with the operating potential window of 0.9 V, between −0.4 and 0.5 V *vs.* Ag/AgCl. Upon exposure to ambient air, reversible redox peaks could be observed in cyclic voltammograms around −0.1 V for samples W5–W48, resembling the peaks observed for the amorphous, mesoporous tungsten oxide.[43]

This result is consistent with XPS measurements indicating the increase of WO_3 concentration on the surface of tungsten oxynitride. It could also be noted that the specific capacitance, measured by galvanostatic charge and discharge tests, increases from 57 F g^{-1} (106 μF cm^{-2}) for the fresh sample (W0) to 75 F g^{-1} (156 μF cm^{-2}) for the sample exposed to air for 48 days (W48). Interestingly, this increase of the capacitance is not accompanied by the fade of the rate capability (Fig. 4b), indicating that the intrinsic conductivity is not affected by the ageing of the samples. In fact, for the fresh sample (W0), 29.6% of the initial capacitance is retained upon increasing the current load from 0.05 to 20 A g^{-1} (400-fold). The exact same

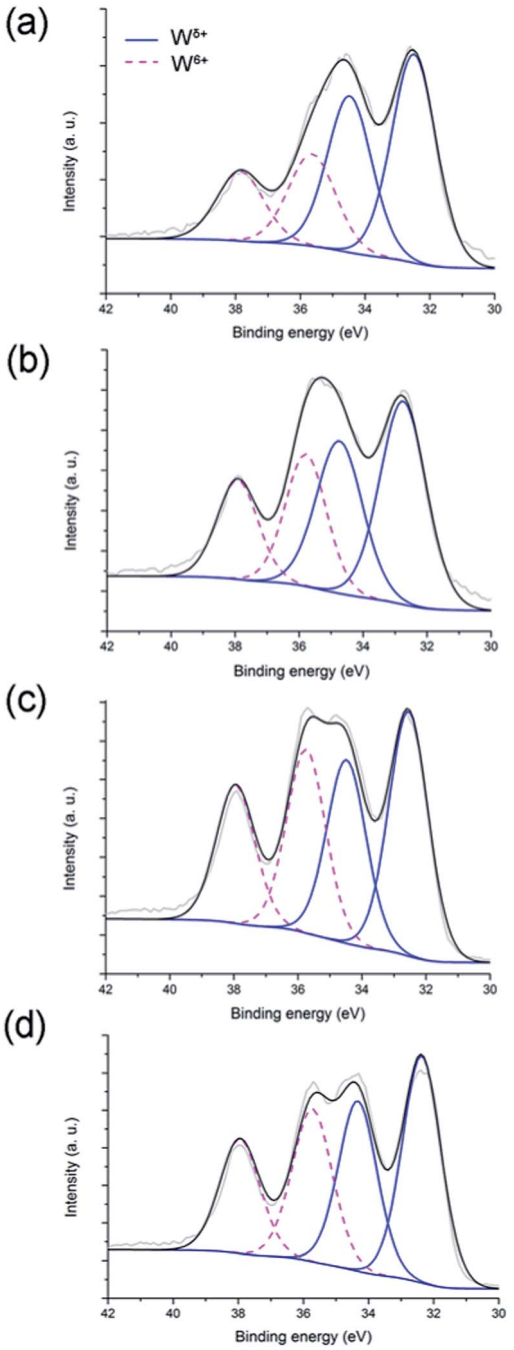

Fig. 2 XPS spectra and W 4f deconvolution peaks for W0 (a), W5 (b), W21 (c) and W48 (d) samples.

Table 3 Binding energies (E_b/eV) of W 4f peaks for samples W0–W48

	W^{6+}		$W^{\delta+}$	
Sample	W $4f_{5/2}$	W $4f_{7/2}$	W $4f_{5/2}$	W $4f_{7/2}$
W0	37.8	35.6	34.5	32.5
W5	37.9	35.7	34.5	32.5
W21	38.0	35.8	34.5	32.5
W48	37.9	35.7	34.3	32.4

Table 4 $W^{6+}/W^{\delta+}$ ratios calculated from the areas of the W $4f_{7/2}$ peaks for samples W0–W48 (Fig. 2)

Sample	$W^{6+}/W^{\delta+}$
W0	0.47
W5	0.75
W21	0.80
W48	0.70

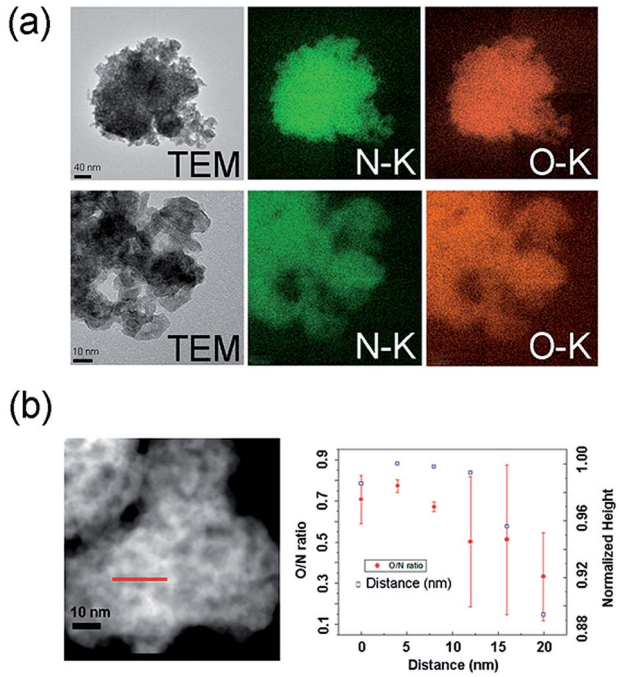

Fig. 3 Bright-field TEM and the corresponding EFTEM maps of O and N elements (a) as well as a high-angle annular dark-field STEM image and the corresponding distribution of the O/N ratio (calculated from the electron energy loss data) along a line scan (in red) (b) for the tungsten oxynitride sample exposed to air for 48 days.

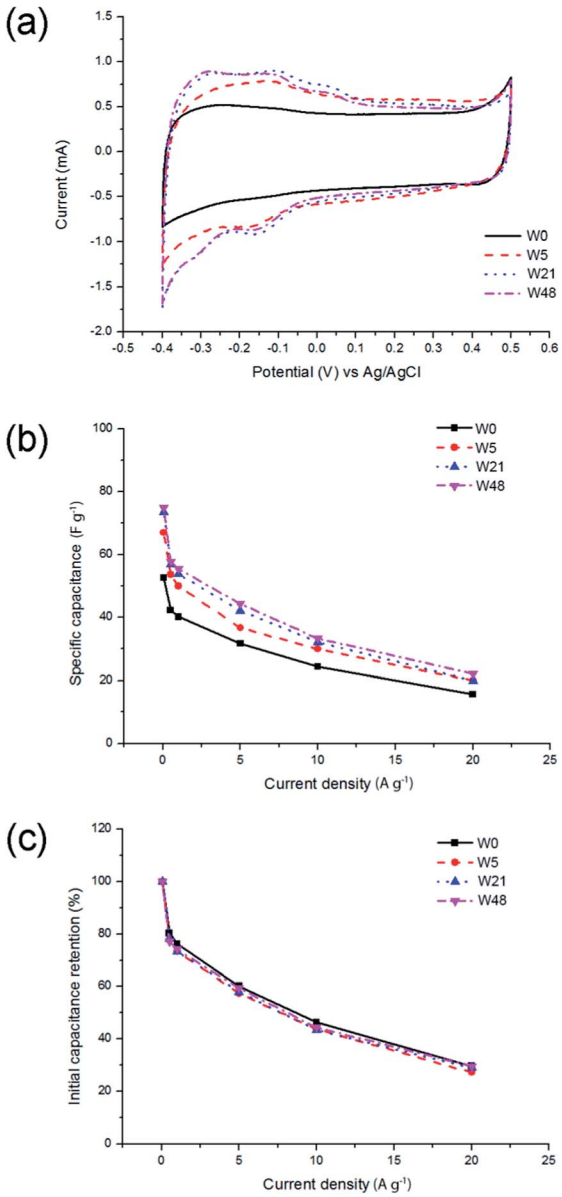

Fig. 4 Influence of ageing on the electrochemical performance of tungsten oxynitrides. Cyclic voltammetry measurements (a), rate capabilities (b) and rate capabilities normalised to the initial capacitance (c) for the fresh and aged tungsten oxynitrides.

value is calculated for the sample exposed to air for 48 days (W48) (Fig. 4c).

The shape of the galvanostatic charge and discharge curves (Fig. 5a) is close to triangular for all samples, with an increased IR drop measured at a higher current load (Fig. 5b). It could, however, be observed that the ageing of tungsten oxynitride leads to a decrease of the Coulombic efficiency, which could be seen from the distortion of the shape of CV curves of the aged samples as well (Fig. 4a). In fact, the Coulombic efficiency calculated from the galvanostatic charge and discharge curves at the current load of 0.05 A g^{-1} decreases from 94% for W0 to only 77% for W48. The changes in the shapes of the electrochemical curves and the decreased Coulombic efficiency may be related to water splitting and hydrogen evolution developing close to −0.4 V *vs.* Ag/AgCl. Overall, it can be concluded that the progressive change of the oxide layer composition over time leads to an increase in the specific capacitance, while the rate capability, which is defined by the conductivity of the sample, remains the same as the bulk of the sample is not affected by the exposure to air. The ageing, however, degrades the Coulombic efficiency, indicating the presence of irreversible processes.

3.1.3 Characterisation of molybdenum oxynitride. N_2 adsorption isotherms for molybdenum oxynitride samples possess a hysteresis (Fig. 6a) and correspond to type IV, typical for mesoporous materials. Surface areas of 123, 39, 60 and 67 m^2 g^{-1} are measured for samples Mo0, Mo21, Mo35 and Mo48, respectively. Interestingly, after the initial drop from 123 to 39 m^2 g^{-1}, an increase of the surface area is observed upon progressive ageing. The maximum of the pore size distribution is centred around 3 nm (Fig. 6b). However, as opposed to tungsten oxynitride, no apparent shift of the maximum is

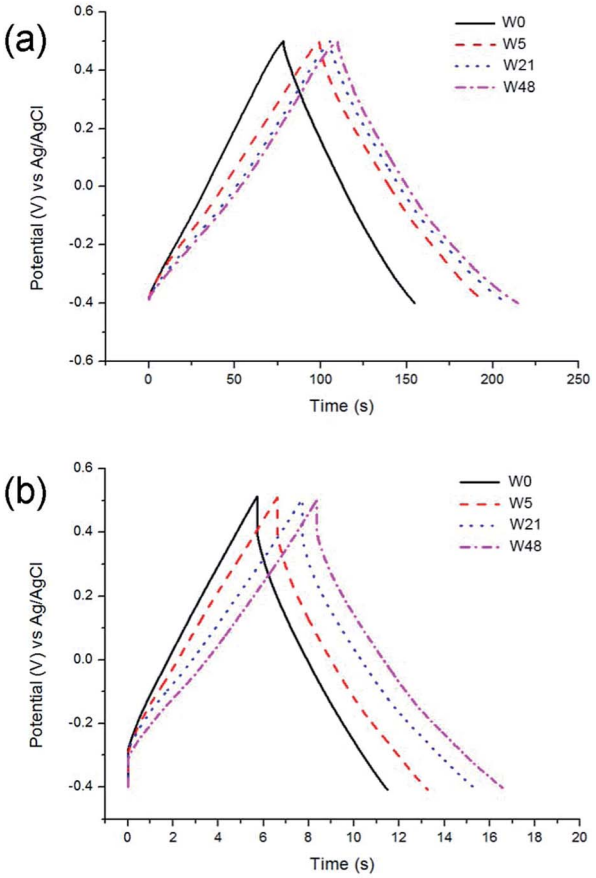

Fig. 5 Glavanostatic charge and discharge curves of tungsten oxynitride samples at the current load of 0.5 A g^{-1} (a) and 5 A g^{-1} (b).

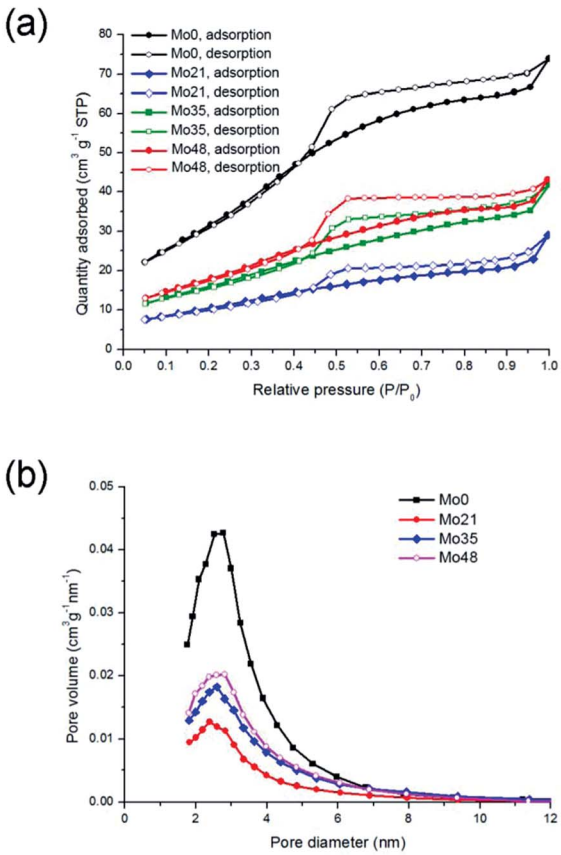

Fig. 6 Nitrogen adsorption and desorption isotherms (a) and pore size distributions (b) for molybdenum oxynitride samples.

observed for molybdenum oxynitride upon exposure of the sample to ambient air.

Mo 3d spectra of the molybdenum oxynitrides are shown in Fig. 7. These, like the W 4f spectra of the tungsten analogues, are fitted with two doublets, with that at higher binding energy having a $3d_{5/2}$ peak centred between 232.4 and 232.7 eV (Table 5). This is within the range of values reported for MoO_3,[44–47] and so the component is assigned to the Mo^{6+} ion. The two peaks of the doublet at lower binding energy have a pronounced asymmetry, with the maximum of the $3d_{5/2}$ component located at 228.7 eV for all four samples. In several previous reports of XPS data acquired for Mo oxynitrides, this asymmetry has been modelled by fitting two peaks, separated by about 1 eV, to each component, and assigning these to additional Mo phases: one containing the Mo^{4+} ion, and another with Mo in a lower, but indeterminate, oxidation state, designated $Mo^{\delta+}$.[47–49] An alternative explanation is that the doublet is associated with a single Mo species, with an oxidation state lower than that of Mo^{VI}, and that the asymmetry is a consequence of multiplet splitting, that is, of the interaction of unpaired 4d electrons with the 3d hole. Such an explanation has been given for the asymmetry observed in the Mo 3d spectrum of MoO_2.[44] Which of these two possibilities properly describes the Mo oxynitrides in this study cannot be resolved from the XPS data alone, and so for the spectra in Fig. 7, each component of the doublet at lower binding energy is fitted with a single asymmetric peak, labelled $Mo^{\delta+}$, representing the contribution from at least one Mo species with $0 < \delta \leq 4$. The $Mo^{6+}/Mo^{\delta+}$ ratios (Table 6) increase for the samples exposed to air, indicating the progressive oxidation, from 0.15 for the sample Mo0 to 0.42 for the sample Mo35. There appears to be no change after 35 days.

3.1.4 Electrochemical properties of molybdenum oxynitride. Electrochemical characterisation of molybdenum oxynitride samples (Fig. 8) shows the operating potentials between −0.5 and 0.5 V *vs.* Ag/AgCl in the 1 M H_2SO_4 electrolyte and multiple redox peaks present on the surface of the cyclic voltammetry curves (Fig. 8a). The maximum specific capacitance of 149 F g^{-1} (121 μF cm^{-2}) is measured for the fresh sample (Mo0) while for the sample exposed to air (Mo48), this value is 152 F g^{-1} (227 μF cm^{-2}), indicating an increase of the specific capacitance per unit of electrode area. As opposed to tungsten oxynitride, the ageing has an effect on the rate capability (Fig. 8b and c). Upon increase of the current load from 0.5 to 20 A g^{-1}, the fresh sample shows a significant drop in the specific capacitance, with only 2.7% of the initial capacitance remaining at 20 A g^{-1} (Fig. 8c). After exposure to air for 48 days, the rate capability increases progressively and reaches 17.2% of the initial capacitance retention for the sample (Mo48).

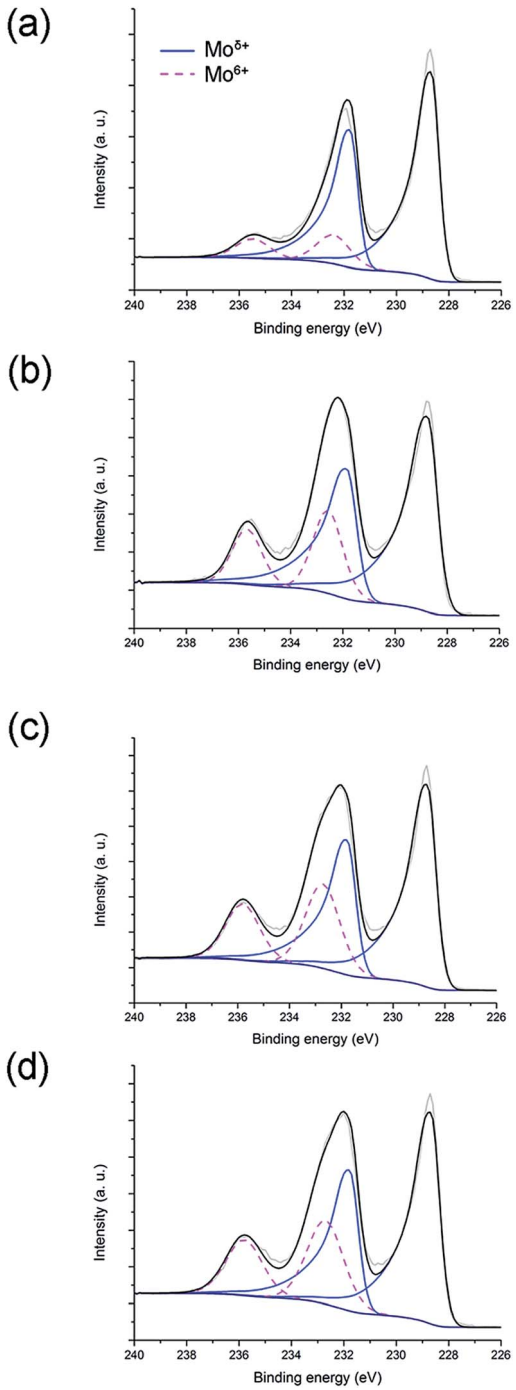

Fig. 7 XPS spectra and Mo 3d deconvolution peaks for Mo0 (a), Mo21 (b), Mo35 (c) and Mo48 (d) samples.

When comparing the shapes of galvanostatic charge and discharge curves of molybdenum oxynitride samples (Fig. 9), no apparent difference is observed at the current load of 0.5 A g^{-1} (Fig. 9a). At the higher current load, however, it can be noted that the IR drop for the aged sample (Mo48) decreases significantly when compared to the fresh sample (Mo0) (Fig. 8 and 9). This could indicate faster kinetics of the electrochemical processes for the sample Mo48.

Table 5 Binding energies (E_b/eV) of Mo 3d peaks for samples Mo0–Mo48

	Mo^{6+}		Mo$^{\delta+}$	
Sample	Mo 3d$_{3/2}$	Mo 3d$_{5/2}$	Mo 3d$_{3/2}$	Mo 3d$_{5/2}$
Mo0	235.5	232.4	231.8	228.7
Mo21	235.7	232.6	231.8	228.7
Mo35	235.8	232.7	231.8	228.7
Mo48	235.8	232.7	231.8	228.7

Table 6 Mo^{6+}/Mo$^{\delta+}$ ratios calculated from the areas of the Mo 3d$_{5/2}$ peaks for samples Mo0–Mo48 (Fig. 7)

Sample	Mo^{6+}/Mo$^{\delta+}$
Mo0	0.15
Mo21	0.33
Mo35	0.42
Mo48	0.42

3.2 Effect of passivation on ageing: comparison of the passivated and non-passivated tungsten oxynitride samples

In order to study the effect of passivation on ageing, passivated tungsten oxynitride samples exposed to ambient air for different periods (WP0–WP48) are characterised by low temperature nitrogen adsorption (Fig. 10) and XPS measurements (Fig. 11). The as-synthesised, passivated tungsten oxynitride sample (WP0) presents a type IV low temperature N_2 adsorption isotherm (Fig. 10a). The maximum of the pore size distribution is, however, shifted towards higher values and is centred around 7 nm (Fig. 10b).

Furthermore, the shape of the isotherm is different from the one reported for samples W0–W48 (Fig. 1). Upon ageing, the maximum of the pore size distribution shifts towards higher values, and reaches approximately 12 nm (Fig. 10b), possibly indicating the blockage of the smaller pores upon room temperature oxidation. The specific surface areas for the samples WP0, WP5, WP21 and WP48, calculated with the BET method, are 44.6, 40.1, 42.3 and 28.5 m^2 g^{-1}, respectively. This decrease in the surface areas, different from the non-passivated samples (Fig. 1), is similar to the previously reported data, where the surface area of the passivated tungsten oxynitride decreased to 30 m^2 g^{-1} after the exposure to air for 40 days.[37] These differences between the passivated and non-passivated tungsten oxynitrides indicate that passivation could have an influence on the structure of the pores.

W 4f spectra of the passivated tungsten oxynitride samples (Fig. 11), like those of the non-passivated samples (Fig. 2), each composed of two doublets, are attributed to W^{6+} and W$^{\delta+}$ (Table 7). The relative ratios of these are listed in Table 8, from which it is evident that this ratio increases steadily with ageing. When comparing the ratios of W^{6+} and W$^{\delta+}$ species for the non-passivated (W0–W48) and passivated (WP0–WP48) samples, it could be observed that for the as-synthesised tungsten oxynitrides, this ratio is slightly lower for W0 (0.47) when compared

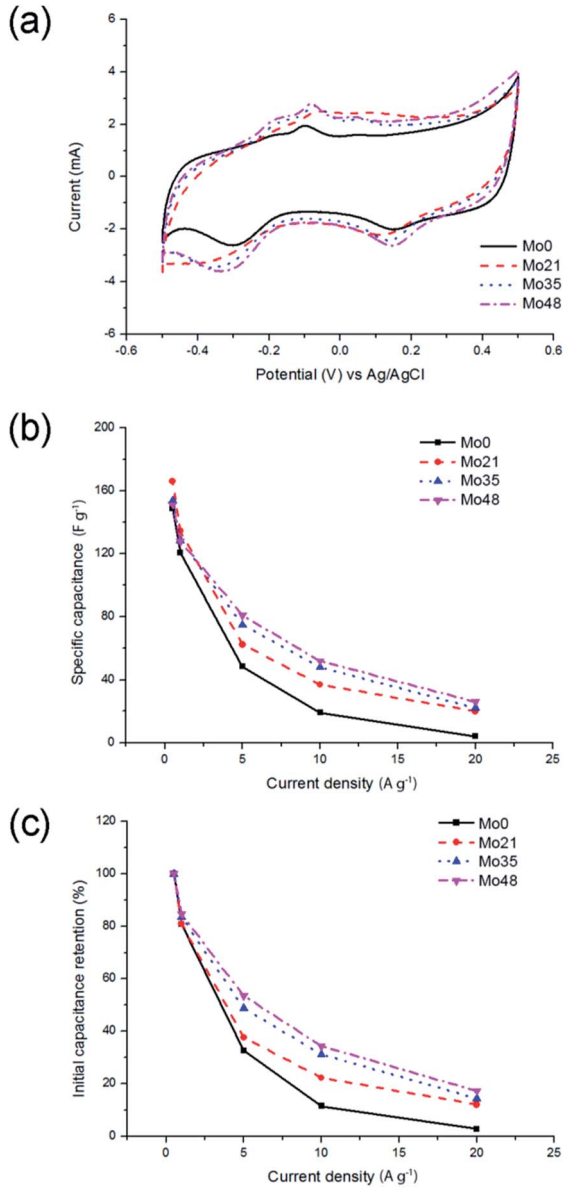

Fig. 8 Influence of ageing on the electrochemical performance of molybdenum oxynitrides. Cyclic voltammetry measurements (a), rate capabilities (b) and rate capabilities normalised to the initial capacitance (c) for the fresh and aged molybdenum oxynitrides.

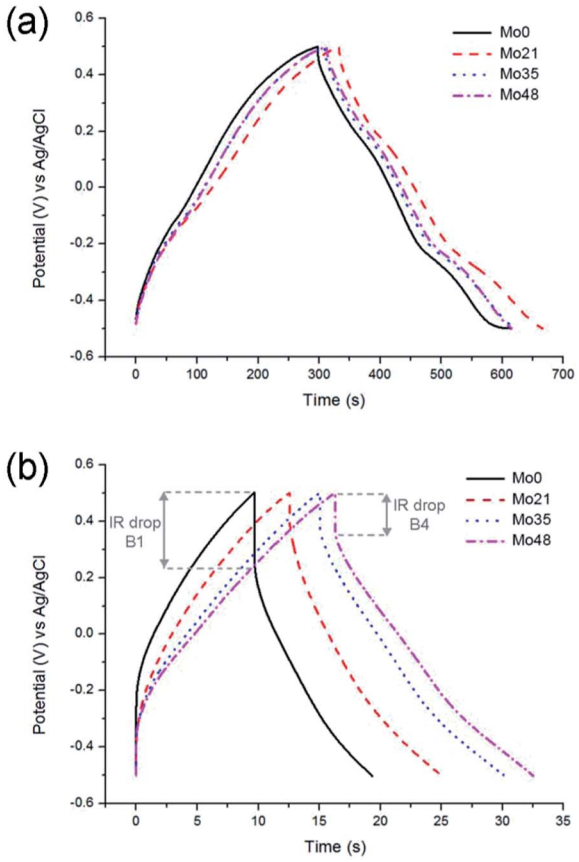

Fig. 9 Glavanostatic charge and discharge curves of molybdenum oxynitride samples at the current load of 0.5 A g^{-1} (a) and 5 A g^{-1} (b). The difference in the IR drop between the fresh (Mo0) and aged (Mo48) samples is highlighted for the higher current load (b).

to that of WP0 (0.49) (refer to Tables 4 and 8). Upon ageing, the $W^{6+}/W^{\delta+}$ ratio for samples W5–W48 increases sharply after the exposure to air for only five days and reaches saturation (Table 4), while for the passivated samples, a progressive increase is observed (Table 8). For samples W48 and WP48 the $W^{6+}/W^{\delta+}$ ratios are 0.70 and 0.76, respectively. These results could indicate that although the passivation of the synthesised tungsten oxynitride slows down the oxidation in ambient air, it does not prevent it.

Cyclic voltammetry measurements of the passivated tungsten oxynitride samples exposed to air for different periods (Fig. 12) indicate a nearly ideal rectangular shape of the CV curves for the freshly synthesised samples. Upon ageing, reversible redox peaks start to appear around −0.1 V, similar to the results observed for the non-passivated samples (Fig. 4a). This distortion of the CV shapes for both passivated and non-passivated materials upon exposure to air correlates with XPS results, and indicates that passivation does not prevent the increase of the amount of tungsten oxide on the surface of the materials, which leads to changes in their electrochemical properties.

When comparing the galvanostatic charge and discharge behaviour of the fresh and aged samples at different current loads (Fig. 13), the curves of the passivated and non-passivated samples nearly superpose at the current load of 0.5 A g^{-1} (Fig. 13a). The specific capacitance values of the as-synthesised samples (W0 and WP0) are 42.3 and 43.6 F g^{-1}, respectively. Upon ageing, the specific capacitance values increase to 57.8 and 58.3 F g^{-1} for samples W48 and WP48, respectively. At a higher current load of 5 A g^{-1} (Fig. 13b), although the as-synthesised, passivated sample (WP0) demonstrates a slightly higher specific capacitance value of 35.6 F g^{-1} when compared to the non-passivated sample (31.7 F g^{-1}), both of the aged samples show similar capacitance values of 44.4 F g^{-1} and 44.2 F g^{-1} for W48 and WP48, respectively.

The progressive changes of the specific capacitance values for the passivated and non-passivated tungsten oxynitride

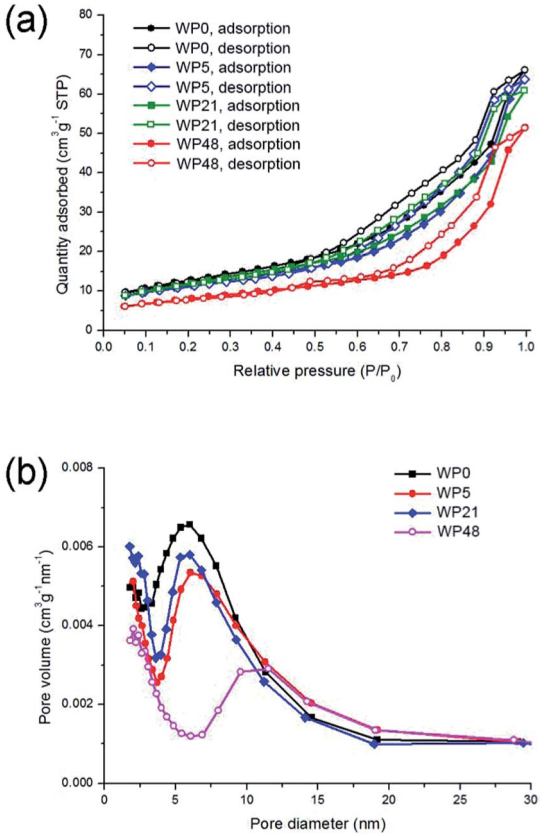

Fig. 10 Low temperature adsorption isotherms (a) and pore size distributions (b) of the passivated tungsten oxynitride samples exposed to air for different periods.

samples with time are depicted in Fig. 14. For the non-passivated samples, a sharp increase of the specific capacitance is observed after five days of exposure to air at the current loads of 0.5 and 5 A g^{-1}, followed by a plateau. For the passivated samples, a different behaviour is observed, with the specific capacitance values increasing progressively with time. After 48 days of exposure, however, both non-passivated and passivated samples reach similar specific capacitance values. These results indicate that the change in the electrochemical properties of the non-passivated samples occurs soon after exposure to air, followed by saturation, while for the passivated samples, this change occurs progressively, thus correlating with XPS measurements.

4. Discussion

Results presented in this work demonstrate that properties of molybdenum and tungsten oxynitrides change with time upon exposure to ambient air. More specifically, an increase of the amount of the oxide species on their surface is observed from the XPS measurements, while changes in the surface areas and pore size distributions are measured with the low temperature N_2 adsorption. The progressive oxidation of the surface leads to significant variations of the electrochemical properties when transition metal oxynitrides are used as active electrode materials for supercapacitors. For instance, for tungsten oxynitrides, although an increase of the specific capacitance is observed upon exposure to air, ageing leads to the distortion of the cyclic voltammetry curves, and decreases the Coulombic efficiencies. For molybdenum oxynitrides, however, an increase of the rate capability is observed. These results indicate that ageing is material-specific and could lead to different consequences: the presence of irreversible electrochemical processes,

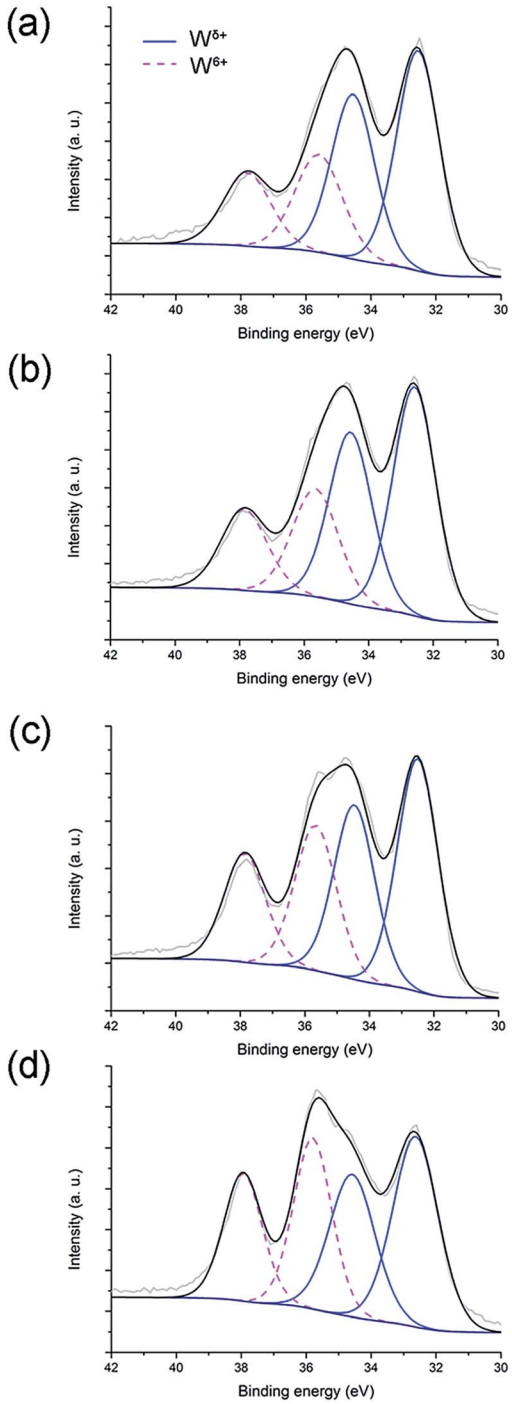

Fig. 11 XPS spectra and W 4f deconvolution peaks for WP0 (a), WP5 (b), WP21 (c) and WP48 (d) samples.

Table 7 Binding energies (E_b/eV) of W 4f peaks for samples WP0–WP48

	W^{6+}		$W^{\delta+}$	
Sample	W $4f_{5/2}$	W $4f_{7/2}$	W $4f_{5/2}$	W $4f_{7/2}$
WP0	37.8	35.6	34.5	32.5
WP5	37.9	35.6	34.6	32.6
WP21	37.9	35.7	34.5	32.5
WP48	37.9	35.8	34.6	32.6

Table 8 $W^{6+}/W^{\delta+}$ ratios calculated from the areas of the W $4f_{7/2}$ peaks for samples WP0–WP48 (Fig. 11)

Sample	$W^{6+}/W^{\delta+}$
WP0	0.49
WP5	0.51
WP21	0.64
WP48	0.76

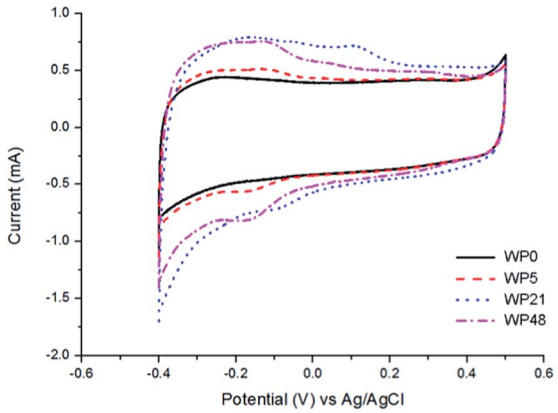

Fig. 12 Cyclic voltammograms of the passivated tungsten oxynitride samples measured with the scan rate of 5 mV s^{-1}.

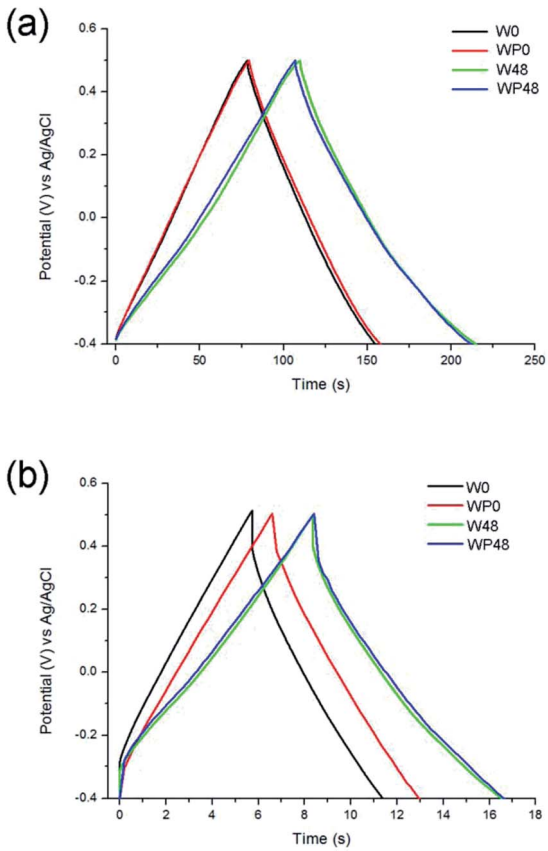

Fig. 13 Comparison of the galvanostatic charge and discharge curves of the non-passivated and passivated tungsten oxynitride samples at the current load of 0.5 A g^{-1} (a) and 5 A g^{-1} (b).

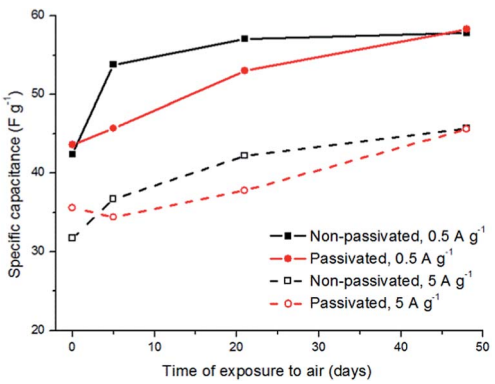

Fig. 14 Comparison of the specific capacitance values for the passivated and non-passivated tungsten oxynitride samples exposed to air for different periods at the current loads of 0.5 and 5 A g^{-1}.

as it is the case with tungsten oxynitride, or an improvement of the rate capability, as it is the case with molybdenum oxynitride. It could therefore be recommended, in view of applications of transition metal nitrides and oxynitrides in the energy conversion and storage devices, to evaluate the influence of ageing on the properties of a specific compound in order to select the optimal storage conditions (controlled ageing or storage in an inert gas atmosphere).

Passivation of transition metal oxynitrides prior to the exposure to air after the temperature-programmed reduction is a common practice, and it is performed in order to avoid the oxidation of the samples. Results presented in this article demonstrate that although passivation has an effect on the properties of the as-synthesised samples and slows down the oxidation in ambient air, it does not prevent the ageing. In fact, after long storage periods, both passivated and non-passivated tungsten oxynitride samples show similar changes in the properties and electrochemical behaviour. It could therefore be suggested to perform passivation when ageing leads to degradation of the electrochemical performance in order to slow down this process.

In summary, results presented in this work demonstrate that passivation prior to exposure to air as well as storage conditions of transition metal oxynitrides has a significant influence on their electrochemical properties. It is therefore recommended

to evaluate and carefully control these parameters when using transition metal oxynitrides in the energy conversion and storage devices. Otherwise, ageing could affect the electrochemical performance, the reproducibility of the measurements, or the comparison of the results to data reported in the literature.

5. Conclusions

In this article, ageing of molybdenum and tungsten oxynitrides is explored and its influence on their electrochemical properties in supercapacitors is investigated. Results indicate that upon ageing, the progressive oxidation of the samples leads to material-specific changes of the electrochemical properties. For tungsten oxynitride, for instance, ageing leads to an increase of the specific capacitance but decreases the Coulombic efficiency, while for molybdenum oxynitride, an improvement of the rate capability is observed. Furthermore, it is demonstrated that although the passivation of the samples prior to the exposure to air slows down the ageing, it does not prevent it. Recommendations are therefore made regarding the preparation and storage conditions of transition metal oxynitrides.

Acknowledgements

This research project was supported by the ARC Centre of Excellence for Functional Nanomaterials, an ARC Discovery grant and a grant from Deakin University (Central Research Grant Scheme). The authors thank Prof Yury Gogotsi (Drexel University) for helpful discussions, Mr Robert Lovett for his help with technical matters and Mr Mengqi Zhou for his help with some figures. The authors acknowledge the use of the XPS facilities in the Victorian Node of the Australian National Fabrication Facility (ANFF).

Notes and references

1 S. Dong, X. Chen, X. Zhang and G. Cui, *Coord. Chem. Rev.*, 2013, **257**, 1946.
2 B. Das, M. V. Reddy, G. V. Subba Rao and B. V. R. Chowdari, *RSC Adv.*, 2012, **2**, 9022.
3 B. Das, M. V. Reddy, G. V. Subba Rao and B. V. R. Chowdari, *J. Mater. Chem.*, 2012, **22**, 17505.
4 B. Das, M. V. Reddy, P. Malar, T. Osipowicz, G. V. Subba Rao and B. V. R. Chowdari, *Solid State Ionics*, 2009, **180**, 1061.
5 B. Das, M. V. Reddy and B. V. R. Chowdari, *Nanoscale*, 2013, **5**, 1961.
6 Q. Sun and Z.-W. Fu, *Electrochim. Acta*, 2008, **54**, 403.
7 Q. Sun and Z.-W. Fu, *Electrochem. Solid-State Lett.*, 2007, **10**, A189.
8 Z.-W. Fu, Y. Wang, X.-L. Yue, S.-L. Zhao and Q.-Z. Qin, *J. Phys. Chem. B*, 2004, **108**, 2236.
9 S. Bouhtiyya, R. Lucio Porto, B. Laïk, P. Boulet, F. Capon, J. P. Pereira-Ramos, T. Brousse and J. F. Pierson, *Scr. Mater.*, 2013, **68**, 659.
10 Q. Sun and Z.-W. Fu, *Appl. Surf. Sci.*, 2012, **258**, 3197.
11 Y.-N. Zhou, C. Liu, H.-J. Chen, L. Zhang, W.-J. Li and Z.-W. Fu, *Electrochim. Acta*, 2011, **56**, 5532.
12 A. M. Glushenkov, D. Hulicova-Jurcakova, D. Llewellyn, G. Q. Lu and Y. Chen, *Chem. Mater.*, 2010, **22**, 914.
13 O. Kartachova, A. M. Glushenkov, Y. Chen, H. Zhang, X. J. Dai and Y. Chen, *J. Power Sources*, 2012, **220**, 298.
14 O. Kartachova, A. M. Glushenkov, Y. Chen, H. Zhang and Y. Chen, *J. Mater. Chem. A*, 2013, **1**, 7889.
15 X. Zhou, C. Shang, L. Gu, S. Dong, X. Chen, P. Han, L. Li, J. Yao, Z. Liu, H. Xu, Y. Zhu and G. Cui, *ACS Appl. Mater. Interfaces*, 2011, **3**, 3058.
16 M. Wixom, L. Owens, J. Parker, J. Lee, I. Song and L. Thompson, in *Proceedings of the Symposium on Electrochemical Capacitors II*, 1997, vol. 96, p. 63.
17 S. Dong, X. Chen, L. Gu, X. Zhou, H. Xu, H. Wang, Z. Liu, P. Han, J. Yao, L. Wang, G. Cui and L. Chen, *ACS Appl. Mater. Interfaces*, 2011, **3**, 93.
18 D. Choi and P. N. Kumta, *J. Electrochem. Soc.*, 2006, **153**, A2298.
19 C. Z. Deng and K. C. Tsai, in *Proceedings of the Symposium on Electrochemical Capacitors II*, ed. M. F. Delnick, Electrochemical Society, Pennington, 1997, vol. 96-25, pp. 75–84.
20 X.-L. Li, Y. Xing, H. Wang, H.-L. Wang, W.-D. Wang and X.-Y. Chen, *Trans. Nonferrous Met. Soc. China*, 2009, **19**, 620.
21 A.-R. Ko, S.-B. Han, Y.-W. Lee and K.-W. Park, *Phys. Chem. Chem. Phys.*, 2011, **13**, 12705.
22 P. Pande, P. G. Rasmussen and L. T. Thompson, *J. Power Sources*, 2012, **207**, 212.
23 X. Zhou, H. Chen, D. Shu, C. He and J. Nan, *J. Phys. Chem. Solids*, 2009, **70**, 495.
24 F. Cheng, C. He, D. Shu, H. Chen, J. Zhang, S. Tand and D. E. Finlow, *Mater. Chem. Phys.*, 2011, **131**, 268.
25 D. Choi and P. N. Kumta, *J. Am. Ceram. Soc.*, 2007, **90**, 3113.
26 D. Choi, G. E. Blomgren and P. N. Kumta, *Adv. Mater.*, 2006, **18**, 1178.
27 M. Wu, Q. Zhang, J. Xiao, C. Ma, X. Lin, C. Miao, Y. He, Y. Gao, A. Hagfeldt and T. Ma, *J. Mater. Chem.*, 2011, **21**, 10761.
28 Y. Wang, M. Wu, X. Lin, Z. Shi, A. Hagfeldt and T. Ma, *J. Mater. Chem.*, 2012, **22**, 4009.
29 G. R. Li, J. Song, G. L. Pan and X. P. Gao, *Energy Environ. Sci.*, 2011, **4**, 1680.
30 Y. Wang, R. Ohnishi, E. Yoo, P. He, J. Kubota, K. Domen and H. Zhou, *J. Mater. Chem.*, 2012, **22**, 15549.
31 P. He, Y. Wang and H. Zhou, *Chem. Commun.*, 2011, **47**, 10701.
32 R. Ohnishi, K. Takanabe, M. Katayama, J. Kubota and K. Domen, *J. Phys. Chem. C*, 2013, **117**, 496.
33 A. Ishihara, S. Doi, S. Mitsushima and K.-I. Ota, *Electrochim. Acta*, 2008, **53**, 5442.
34 H. Tominaga and M. Nagai, *Electrochim. Acta*, 2009, **54**, 6732.
35 C. Pozo-Gonzalo, O. Kartachova, A. A. J. Torriero, P. C. Howlett, A. M. Glushenkov, D. M. Fabijanic, Y. Chen, S. Poissonnet and M. Forsyth, *Electrochim. Acta*, 2013, **103**, 151.

36 K. Zhang, L. Zhang, X. Chen, X. He, X. Wang, S. Dong, P. Han, C. Zhang, S. Wang, L. Gu and G. Cui, *J. Phys. Chem. C*, 2013, **117**, 858.
37 D.-H. Cho, T.-S. Chang and C.-H. Shin, *Catal. Lett.*, 2000, **67**, 163.
38 X. Goin, R. Marchand, P. L'Haridon and Y. Laurent, *J. Solid State Chem.*, 1994, **109**, 175.
39 C. Sayag, G. Bugli, P. havil and G. Djéga-Mariadassou, *J. Catal.*, 1997, **167**, 372.
40 M. R. Lukatskaya, O. Mashtalir, C. E. Ren, Y. Dall'Agnese, P. Rozier, P. L. Taberna, M. Naguib, P. Simon, M. W. Barsoum and Y. Gogotsi, *Science*, 2013, **341**, 1502.
41 *Handbook of X-ray Photoelectron Spectroscopy*, ed. J. Chastain, Perkin-Elmer Corp., Minnesota, USA, 1992.
42 J. F. Morar, F. J. Himpsel, G. Hughes, J. L. Jordan and F. R. McFeely, *J. Vac. Sci. Technol., A*, 1985, **3**, 1477.
43 C. Jo, I. Hwang, J. Lee, C. W. Lee and S. Yoon, *J. Phys. Chem. C*, 2011, **115**, 11880.
44 F. Werfel and E. Minni, *J. Phys. C: Solid State Phys.*, 1983, **16**, 6091–6100.
45 L. D. Lopez-Carreno, G. Benitez, L. Viscido, J. M. Heras, J. M. Yubero, J. P. Espinos and A. R. Gonzalez-Elipe, *Surf. Interface Anal.*, 1998, **26**, 235.
46 C.-O. A. Olsson, H.-J. Mathieu and D. Landolt, *Surf. Interface Anal.*, 2002, **34**, 130.
47 Z. B. Wei, P. Grange and B. Delmon, *Appl. Surf. Sci.*, 1998, **135**, 107.
48 Y. Zhang, Q. Xin, I. Rodriguez-Ramos and A. Guerrero-Ruiz, *Mater. Res. Bull.*, 1999, **34**, 145.
49 J.-G. Choi, J. R. Brenner, C. W. Colling, B. G. Demczyk, J. L. Dunning and L. T. Thompson, *Catal. Today*, 1992, **15**, 201.